Sub-GHz linewidth ensembles of SiV centers in a diamond nano-pyramid obtained by persistent hole burning

Louis Nicolas, Tom Delord, Paul Huillery, and Gabriel Hétet*

Laboratoire de Physique de l'Ecole normale supérieure, ENS, Université PSL, CNRS, Sorbonne Université, Université Paris-Diderot, Sorbonne Paris Cité, Paris, France.

E-mail: gabriel.hetet@lpa.ens.fr

Abstract

Producing nano-structures with embedded bright ensembles of lifetime-limited emitters is a challenge with potential high impact in a broad range of physical sciences. Amongst those emitters, SiV centers in diamonds have unique optical properties which makes them ideal for this objective. In this work, using a combination of resonant photo-luminescence excitation and a frequency-selective persistent hole burning technique, we demonstrate close to lifetime-limited emission from high density ensembles of SiV centers in a diamond nano-pyramid grown by chemical vapor deposition. Compared to hole burning methods that use orbital states for shelving or two-level atom saturation techniques, the employed hole burning uses controlled charge transfer to and from dark states exhibiting very long lifetimes. We suggest a mechanism involving nitrogen impurities that explains our observations. Such a nanostructure with thousands of bright close to lifetime-limited emitters in a volume much below λ^3 will be useful for studies of super-radiance, for biological sensing, and nanoscale thermometry.

Photoluminescent defects in diamond are atom-like systems in the solid state that have unique photo-physical properties. Most of them indeed feature stable and bright photoluminescence (PL) at room temperature, making them ideal single photon sources. In particular, the electronic spin of the negatively charged nitrogen vacancy (NV^-) defect can be manipulated at room temperature, used to probe magnetic and electric fields, as well as nearby nuclear spins, and to realize a temperature and strain probe.[1] Another defect, the negatively charged silicon vacancy center (SiV^-) has also received considerable interest over the past decade. One advantage of the SiV^- center over the NV^- center is that most of its photoluminescence concentrates in the zero-phonon line. Moreover, SiV centers provide optical qubit states with coherence times exceeding 10 ms at temperatures below 500 mK.[2] Another advantage of the SiV centers spectral lines is that they are almost insensitive to nearby charge fluctuations,[3] due to their inversion symmetry, which leads to a narrow inhomogeneous broadening.

For many applications in sensing, labeling and quantum information, using color centers within nanostructures and nanodiamond (NDs) is essential to incorporate them into cells or use them for scanning probe-based sensing. Using NDs also means more efficient collection of their PL. Incorporating ensembles of SiV centers into diamond nanostructures while remaining close to the lifetime limit is challenging because preserving the axial symmetry is a difficult task. Indeed, in NDs, strain breaks the axial symmetry, which makes the centers very sensitive to surface charge fluctuations and in turn increases the spectral diffusion. There is however great progress in this direction. Single SiV^- centers in CVD grown nanodiamonds have exhibited 20 GHz linewidths, limited by spectral diffusion.[4] Single SiV centers with lifetime limited linewidth (approx. 100 MHz) has already been achieved in diamond nanostructures using implantation[5] or via plasma etching.[6,7] Single SiV centers in nanodiamonds grown via a high-pressure high-temperature method and subsequently treated in hydrogen plasma have also exhibited very close to lifetime limited linewidths (354 MHz).[8] The static spectral shifts due to strain are however typically very large in nanostructured diamonds. It

can be turned into an advantage since single SiV can be spectrally isolated, however, this precludes reaching the lifetime limit when using ensembles of SiV centers in nanostructure. In this work we will use CVD grown low-strain nano-pyramids together with charge state conversion as a means to counteract this issue.

For most defects in diamonds, charge state conversion plays an important role. It can lead to an overall decay of the PL and can necessitate laser pulse sequences for repopulating the desired charged states. Conversely, charge state conversion can have advantages. It was for instance used to demonstrate detection of the NV^- electronic spin state[9] and lead to the development of ground-state depletion microscopy (GSD)[10] and persistent hole burning.[11,12] As in the case of NV centers, switching the charge state of the SiV was also observed[13] and used to manipulate single SiV^- centers.[14] Further, as opposed to the NV center, the neutral form of the SiV center has impressive spin properties.[15]

In this work, we first demonstrate optical and fatigue-free charge state control over a high density of SiV centers located at the apex of a diamond nano-pyramid. We then use resonant photo-luminescence excitation in conjunction with persistent hole burning to show close to lifetime-limited emission of thousands of bright emitters in a volume below λ^3.

The samples that we employ are CVD grown Artech Carbon AFM tips. These samples were investigated in Ref. 16–18 where ensembles of SiV^- centers located at the ten nanometer size apex of the tip already show inhomogeneous broadening that is less than 10 GHz.[17] We have two different types of samples at our disposal : pyramids containing nitrogen impurities and pyramids where no nitrogen was detected. Both contain SiV centers mostly at the apex.[17] In the present study, we mainly study the first sample. The pyramids are deposited on quartz or silicium substrates as depicted in Fig. 1-a). To study their PL properties, we use the same homebuilt confocal microscope working at cryogenic temperatures as in Ref. 17 and now add a laser tuned to the 737 nm zero-phonon line.

The nitrogen concentration of the diamond nano-pyramids under study is 10 ppm.[16] A significant fraction of the photoluminescence is also emitted by NV centers. An optical

spectrum measured at the apex of the pyramids is shown in Fig. 1-b). It has been obtained at 6K, using 4 mW of green laser excitation focused on the sample by a 0.25 numerical aperture objective, and taken on a 1200 lines/mm grating spectrometer. The zero-phonon line (ZPL) of both the NV^- and SiV^- centers are observed at 637 and 737 nm respectively. The spectrum also features the phonon sidebands (PSB) of both centers. The NV center's PSB ranges from 645 nm to 730 nm. Due to a similar symmetry between the SiV ground and excited states, the SiV center's coupling to the phonons is much weaker than that of the NV center, so the relative area under its PSB is much smaller. It extends from 740 to 765 nm, and also features the local silicium oscillation mode at 763 nm.[19]

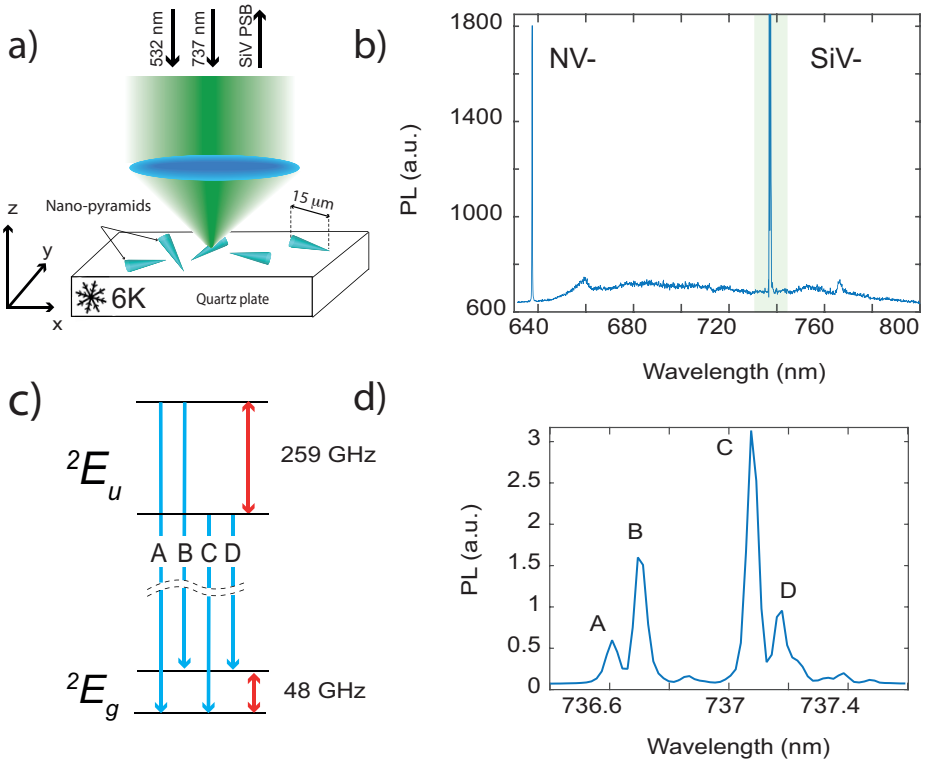

Figure 1: a) Schematics of the confocal microscope set-up, showing nano-pyramids deposited on a quartz plate, and the two employed lasers at 532 nm and 737 nm. b) Optical spectrum of the photoluminescence (PL) emitted by the pyramids in the 630 to 800 nm range. c) Level scheme of the SiV^- center. d) PL spectrum close to the SiV center, showing the four characteristic ZPLs under green excitation. The smaller other peaks correspond to the photoluminescence from other silicon isotopes.

Using a narrow band filter around the SiV^- ZPL, we found photoluminescence rates of

around 1 million counts per seconds with 1 mW of green laser light. This very high count rate implies a high SiV concentration, considering the fairly small numerical aperture (NA=0.25) that we use in the experiment and the fact that most of the emission is funneled through the diamond tip.[18]

A zoom on the SiV^- ZPL is plotted in Fig.1-d). The four characteristic ZPL transitions of the SiV^- are observed together with smaller peaks corresponding to the photoluminescence from other silicon isotopes. The two ground and excited states are splitted by 48 GHz and 259 GHz respectively due to spin-orbit coupling. Observing such a bulk-like SiV^- spectral response with ensembles of SiV^- centers already underlines the very small strain in the nano-pyramid.

Photoluminescence excitation (PLE) using a laser that is scanned about the ZPL is an efficient method to obtain an even higher spectral resolution. In PLE experiments with SiV centers, a resonant laser beam at 737 nm is scanned close to the SiV ZPL, and the PL is collected on the phonon side band (PSB) after filtering the laser light using a longpass filter.

In our first attempts to do so, we observed no PL on the PSB. However, when the green laser is present, the resonant laser could increase the PL. Fig. 2-a) shows a typical time trace where the photoluminescence rate in the 750 and 770 nm range is plotted for 18 s during which green and red lasers are turned on and off and kept at optical powers of 4.3 mW and 9.5 μW respectively. Their wavelengths are 532 nm and 737 nm respectively. When the green laser is turned on, a count rate of 520 kcounts/s is measured. This count rate is stable for hours. Here, we then turn on a red laser at a time t=2.6 seconds. The count rate then increases to 830 kcounts/s, with also similar long term stability. When turning off the green laser, at a time t=6s however, the photoluminescence of the SiV^- center is completely suppressed. This dark state can be switched again back on by applying a laser at 532 nm. We repeated the same procedure and measured the same photoluminescence rates by applying the green and red sequence again. Crucially, this effect is only seen when using pyramids that contain nitrogen. When doing similar sequences with nitrogen free pyramids, the PL

is still present under red excitation, even if the green laser is turned off. This observation points towards a decisive role played by nitrogen impurities.

There is also no trapping into the dark state in the absence of illumination even after letting the system evolve in the dark during hours. We also measured that the lifetime of the dark state is more than one hour and that the trapping process occurs also with laser wavelengths above 630 nm at room temperature. As we will explain in the following, this "dark" period is due to a charge state conversion of the SiV center.

To gain more insight into the nature of this charge state transfer process, we recorded the PL counts as a function of green and red laser powers. Fig. 2-b), left, shows the PL rate as a function of the green laser laser power for up to 5 mW, in the absence of red laser. The linear dependence of the PL with respect to the green laser demonstrates that the SiV centers optical transitions are not saturated. The figure on the right shows the PL count rate as a function of the resonant laser power from 0 to 2 μW, with the green laser power set to 4.12 mW. Here again, the PL increases linearly for up to 1 μW so the SiV transition is not saturated below this power level. This points are important in order to understand the nature of the charge transfer processes.

We then measured the photoluminescence decay time after shining the red laser. This measurement is done without green laser light, for modest red-laser powers (2.1μW), after having prepared the SiV^- centers using green excitation. As shown in Fig. 3-a), we turn on the resonant laser at time $t = 0s$ and monitor the photoluminescence decay. We see that it takes place on time scales of about 100 ms. This means that the dynamics is governed by photoionisation towards the conduction band and not by direct optical excitations, the latter typically taking place on nanosecond time scales. Importantly, no plateaus in the decay curve are observed which again highlights the very high SiV center concentration. The solid lines are a fit using the model that we describe next.

The charge conversion process occurs through photo-ionisation. This is indeed a common mechanism in diamond, which has been extensively studied in the NV^- center.[10,20–24] These

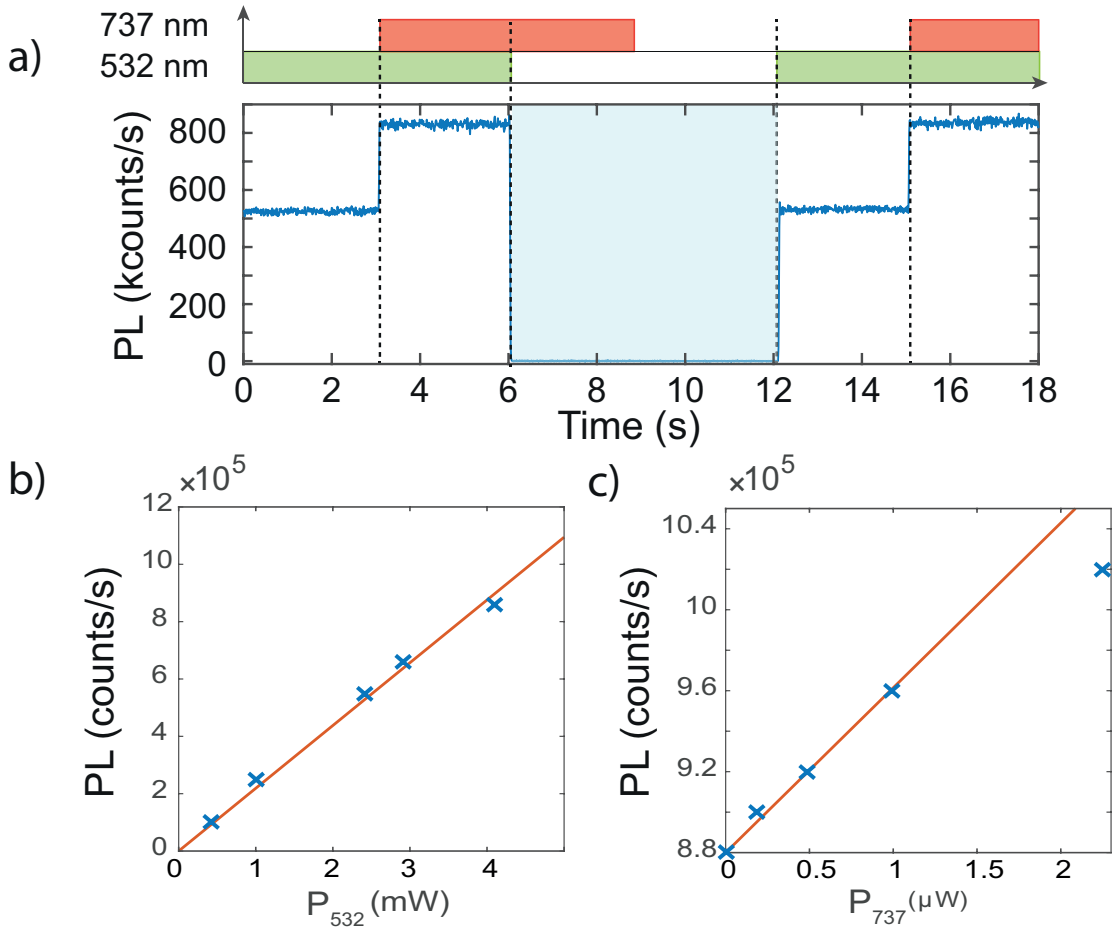

Figure 2: a) Illumination sequence used to reveal the trapping of the SiV center into the dark state. The power of the green and resonant lasers are $P_{532} = 4.3\mu W$ and $P_{737} = 9.5\mu W$. b) Left : PL count rate as a function of green laser power (with the resonant laser off). Right : PL counts as a function of the resonant laser power, with the green laser power set to 4.12 mW.

previous works show that the NV^- centers can be ionized under resonant excitation (637 nm) via a two photon process. First, a photon promotes the NV^- in its excited state and a second photon brings the electron to the diamond conduction band. This process forms NV^0 states plus one electron that is trapped by another impurity. The NV^0 center, the neutral NV form, can then be converted back into the NV^- under green excitation : First, a photon brings the NV^0 in its excited state. Then an other photon promotes a valence electron (coming from the deep lying NV^0 a_1 orbital) to its fondamental state. The hole migrates away from the center which is now in its negatively charged state.

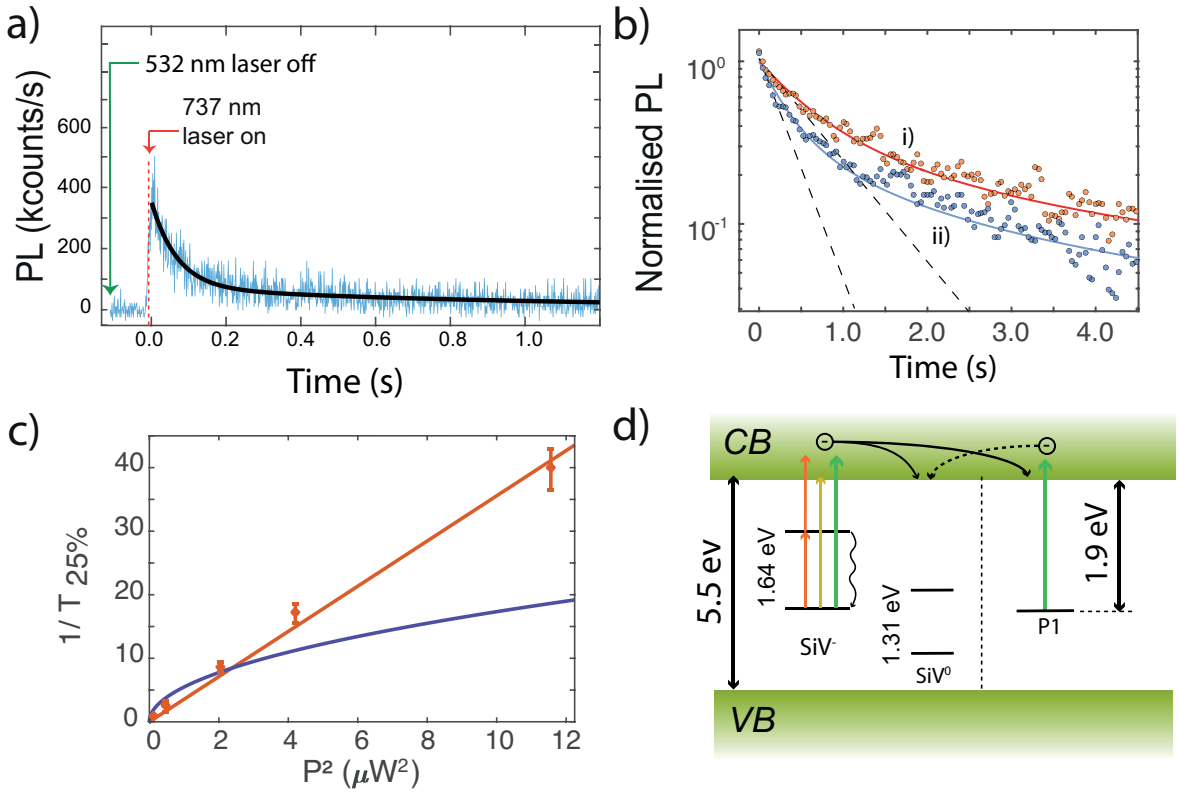

Figure 3: a) Blue curve: photoluminescence as a function of time when the resonant laser is turned on. Background has been removed. The power of the resonant laser is $P_{737} = 2.1\mu W$. The black curve is a fit of the photoluminescence under resonant excitation. b) Photoluminescence rate as a function of time on a log scale, for two different, and weaker, resonant laser powers. c) characteristic decay rate as a function of the square of the power of the resonant laser. In red, the linear fit highlights the two photon behavior. The blue line corresponds to a fit using a linear dependence with laser power. d) Valence and conduction bands and energy levels of the SiV centers and P1 centers inferred from the measurements.

The charge transfer dynamics between the SiV^- center and its neutral state, the SiV^0 center, is however still being investigated. Let us now formulate our hypothesis : under resonant excitation, an electron already in the SiV^- excited state can be promoted to the conduction band. Thus, the SiV^- is converted into SiV^0. Then, the electron diffuses and is captured by impurities. If only SiV are present in the diamond, the electron is captured by the SiV^0 which returns to its charged state. Indeed, it is admitted that SiV^0 can recombine with an electron of the conduction band.[13] That could explain why the PL is stable under resonant excitation when no nitrogen is present, as we experimentally checked. If nitrogen is present in the diamond however, the electron can be trapped by a P1 center to form

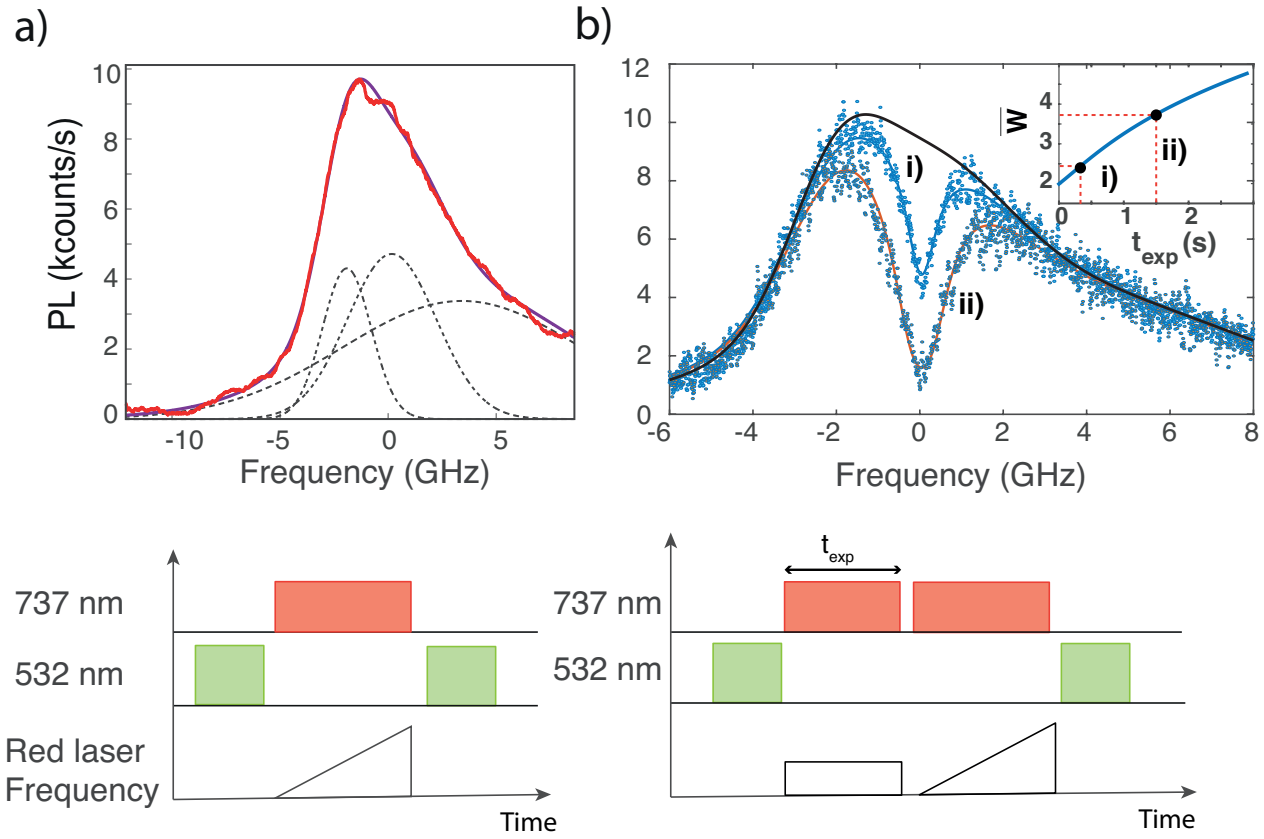

Figure 4: a) Averaged PLE measured by scanning the resonant laser at 737 nm around transition C, in the presence of green laser light between scans. b) PLE spectra after three different exposure times at 6K : in black without hole burning, in blue $t_{exp} = 300$ ms and in orange, $t_{exp} = 1500$ ms. The dots represent raw data and the continuous lines are fitted data. Here $P_{737} = 0.877\mu W$. The inset shows the width $\overline{W}$ of the holes inferred from the fit and normalized to the homogeneous linewidth Γ_e ($\overline{W} = \Gamma_h/\Gamma_e$). Notice the factor of two between the hole width and the homogeneous linewidth Γ_e when t_{exp} tends to zero.

a negatively charged P1 center.[25] This defect can further be photo-ionised using a more energetic excitation, such as with green light.

In our experiment, the total loss of PL suggests that the nitrogen concentration of our sample is high enough to trap all the electrons coming from photoionisation of SiV^- centers into P1 defects. This process is schematized in Fig. 3 d). It is important to stress upon the ability of the neutral SiV to efficiently capture an electron for being converted to the charged state. That is why this trapping effect occurs only when other defects are present and are able to trap the electrons, whereas the control of the charge state of the NV center does not

require other defects. The fact that this optically controlled charged state switching is not seen on samples free of nitrogen confirms this hypothesis, which was already formulated in Ref. 26, and is in accordance with Ref. 13.

Similarly to SiV^-, the neutral charge state emits the majority of its photons at the zero-phonon line (ZPL) at 946 nm (1.31 eV). In this work, we could not observe the SiV^0 center photoluminescence using laser excitations at wavelengths of 532, 737 and 800 nm. This can be both the result of our poor detection efficiency at 946 nm and due to the presence of a state that decays non-radiatively. It may be observed by pinning the Fermi level such that the neutral charge state has the lowest formation energy.[15] Fermi level engineering in diamond however requires careful control of other structural and point defects, which is difficult when nano-structures are used. Indeed, the presence of surface defects significantly complicates the analysis of the charge transfer dynamics.

Let us now characterize the rate of the state conversion process further. Fig. 3-b) shows the photoluminescence rate as a function of time on a log scale, for two different resonant laser powers : P_{737}= 347 nW and 683 nW for traces i) and ii) respectively. The decay process features two long time scales, a shorter one, in the hundreds of millisecond range, and a longer one, in the tens of second range. These two time-scales are the result of excitation of an inhomogeneous class of emitters: the emitters which are exactly at resonance are trapped into the dark state faster than ones which are detuned. The short (resp. long) times scale thus correspond to the population dynamics of resonant (resp. off resonant) emitters. in accordance with the model described below.

The characteristic faster decay rate is also plotted as a function of the square of the power in Fig. 3-c). The decay rate plotted on the y axis is the inverse of the duration needed to lower the PL by 75%. A linear dependence of the decay versus the square of the laser power reveals the two-photon nature of the fast excitation process, as described by the level scheme shown in Fig. 3-d). Another fit, the blue line, corresponds to a fit using a linear dependence with laser power, which does not agree with the data. Since we do not saturate the SiV

center at these power levels (as shown in Fig. 2-b), a linear power dependency of the decay rate would be associated with single photon process, whereas quadratic dependency reveals a two photons transition. It confirms that two resonant photons are needed to promote an electron from the fundamental SiV^- state to the conduction band and implies a energy gap between the SiV^- center and the conduction band that is less than 1.64 eV. Further work will be done in order to understand the discrepancy that exists between this explanation and the *ab initio* calculations that show that the SiV^- excited state lies much closer to the valence band.[27,28] This two-photon process is not seen on every pyramids however. Around 75% of the dozen of studied pyramids show this dependence, the other show a linear dependence with power, which may then stem from a saturation of the transition between the excited state of the SiV^- to the continuum.

Having observed and analyzed this charge transfer mechanism, we now come back to resonant PLE. To perform PLE, the resonant laser power and scan durations are now chosen in order to ensure that the illumination duration is shorter than the PL loss timescale. As shown in Fig. 4-a) a green laser is turned on before and after the scan. The PLE spectrum is the accumulation over several scans separated by a green laser illumination so as to recover the PL signal. A typical PLE scan around transition C is shown in Fig. 4-a) and features similar asymmetrical profiles than the ones observed in Ref. 17 using a Fabry-Pérot cavity. Here, a minimal fit to the PLE spectra is found by using three displaced Gaussian curves of varying widths. These are the dashed lines in Fig. 4-a). Although the overall width of the PLE spectrum is found to be 7 GHz, this fit suggests that the spectrum is comprised of several emitters of varying width and central position. Let us give a tentative interpretation to the fit that we obtain. Axial strain shifts the line center of the $SiV-$ center towards to high wavelengths, whereas transverse strain shifts all the frequency to the blue.[29] Since all 4 SiV lines feature a tail dragging to high frequency, a possible effect is that the ensemble of SiV at lower frequency experience a more homogeneous axial strain. The SiV centered at 5 GHz may be at another more strained position in the sample, and experience a broader

strain distribution. One may stem from the original HPHT seed. The other may come from the CVD in the growth process. A more realistic model would include more families with widths continuously increasing towards high frequencies. An other explanation could be the presence of a strain gradient together with an SiV concentration gradient. The density is higher at the apex of the tip where the strain is fixed by the seed crystal. Going to the base of the pyramid, the strain would continuously change to the value specific to the CVD bulk while the concentration decreases.[16]

Since the PLE signal comes from the sum of homogeneous lines from emitters having different ZPL frequencies, hole burning techniques may be employed to access spectral features beyond the inhomogeneous width. Hole burning ensembles of SiV centers was demonstrated in Ref. 30 where one other resonant laser saturated one class of emitters. Here, we use the frequency dependence of the dark state trapping to show persistent hole burning.

The sequence is depicted in Fig.4-b). After a short green illumination to ensure that the SiV centers are in the bright state, the sample is exposed to resonant light at a fixed frequency at the center of the inhomogeneous profile $\nu = 0$ during a time t_{exp}. The frequency of the resonant laser is then scanned over tens of GHz around the central frequency during 100 ms, shorter than the characteristic transfer rate to the dark state. The photoluminescence is recorded during the scan. To obtain a high enough signal to noise ratio, another green laser pulse is applied after the scan, and the sequence is repeated. The resulting spectra are plotted in Fig 4-b). As expected, the PLE spectra now feature holes within the inhomogeneous profile, centered at a frequency $\nu = 0$ and with widths that depend upon the exposition time t_{exp}. The data are well fitted by a model that we present in the SI.

This charge state conversion therefore allows us to perform efficient persistent spectral hole burning, which gives access to the homogeneous linewidth. The measured estimated homogeneous width is 390 ± 12 MHz, which is only 2.8 times greater than the homogeneous width obtained in bulk samples.[3] Further work will be conducted to estimate the contribution of spectral diffusion on the obtained width, but our results already show that it is very small

in such nano-pyramids, which opens perspectives for preparing narrow spectral features containing many SiV^-.

In conclusion, we have demonstrated close to lifetime-limited emission from a high density ensemble of SiV centers in a diamond nano-pyramid at cryogenic temperature. We have done so using resonant photo-luminescence excitation in conjunction with persistent hole burning. We have also shown that impurities that are electron acceptors needs to be present in the diamond to enable SiV charge state control. In our sample, we believe that the nitrogen concentration is high enough to optically trap all the SiV centers in their neutral state and so to cancel out all the SiV^- photoluminescence.

Optical control of the SiV charge state has already found applications. It is for instance used to isolate a single SiV^- center putting all the other in the neutral state.[14] The hole burning we use is unique in that it is fatigue free and is all optically controlled via a long lived dark states so the technique can be used to create regular spectral patterns that could then be used for light storage, using the atomic frequency comb technique.[31] At present the lifetime of the ground orbital states is most likely limited both by the coupling to impurities and by photons. Using spin echoes and using a dilution fridge to reach mK temperatures could then enable SiV ensembles to be used as an efficient quantum memory for light with long coherence times.

Finally, at room temperature, this effect could also lead to applications for biological imaging. Combining ground state depletion microscopy (GSD) (already performed with NV centers[10]) and diamond bio-imaging techniques[32] can enable sub-wavelength resolution.

We would like to thank Elke Neu, Vincent Jacques and the nano-optics team at LPENS for fruitful discussions and Romaric Le Goff for technical assistance. GH acknowledges funding by the French National Research Agency (ANR) through the project SMEQUI and by the T-ERC program through the project QUOVADIS.

Supplementary Information

To describe the dynamics of the hole burning technique, we present a model that starts with a spectral distribution of emitters given by the PLE spectrum and assume that they all have the same spectral linewidth Γ_e. We assume that the recombination time of the electrons promoted to the conduction band is faster than all the other phenomena at play. We assume that the rate of excitation from the excited state to the conduction band $a\Phi$ is much weaker than the excitation rate on the ZPL. In that case, the rate of loss of SiV^- centers at the frequency ν_0 as a function of time under excitation at the frequency ν_{exc} with a photon flux Φ is given by

$$a\Phi \times \frac{b\Phi}{\frac{\Gamma_e^2}{4} + (\nu_0 - \nu_{exc})^2}$$

where the first term of the product is the excitation from the excited state to the conduction band rate, and the second term corresponds to the excitation rate of the SiV^- on the ZPL transition. This last expression is justified by our observations that the SiV ZPL transition is not saturated with the low red laser powers that we use. This equation predicts that the number of bright emitters depends on the square of the optical power under the above assumptions. The overall photoluminescence under excitation at the frequency ν after exposition to the frequency ν_{exc} during a time t is then the sum of the contribution from all SiV− centers.

$$\mathrm{PLE}(\nu, t) \propto \int_{-\infty}^{\infty} \frac{d(\nu_0)}{\frac{\Gamma_e^2}{4} + (\nu_0 - \nu)^2} e^{-\Phi^2 \frac{ab}{\frac{\Gamma_e^2}{4} + (\nu_0 - \nu_{exc})^2} t} d\nu_0, \tag{1}$$

where $d(\nu_0)$ is the spectral distribution of the emitters.

Using to this model, we can compute the PLE decay at fixed excitation wavelength. We used it to predict and fit the change in the PL as a fonction of time under resonant excitation, in the experimental traces shown in Fig. 4 and Fig. 3.

We also used this model to fit the hole burning spectra presented in Fig. 4. To accurately estimate the homogeneous broadening of our sample, we acquire several hole burning spectra

at the same laser power, but with different exposure times. To fit these data with the model, we use three parameters: $C_1 = \Gamma_e$, $C_2 = \Phi^2 abt$ and $C_3 = \nu_{exc}$. We fit at the same time all the four spectra of the series. We thus have a set of six parameters to optimize: C_1, C_3 and four C_2. To check the validity of this procedure, we verify that the parameter C_2 is linearly dependent with the exposure time. This leads to the estimation of Γ_e which is here 390 ± 12 MHz.

Importantly, according to this model, the linewidth of the hole cannot be lower than twice the homogeneous linewidth. This can be seen by assuming a small interrogation time and doing the Taylor expansion

$$\mathrm{PLE}(\nu, t) = A + B \int_{-\infty}^{\infty} \frac{1}{\frac{\Gamma_e^2}{4} + (\nu_0 - \nu)^2} \frac{1}{\frac{\Gamma_e^2}{4} + (\nu_0 - \nu_{exc})^2} d\nu_0 \tag{2}$$

where A and B are independent on frequency. This corresponds to the convolution of two Lorentzian fonctions. The result is then a Lorentzian fonction with a width that is twice as large as the initial Lorentzian widths.

References

(1) Bernardi, E.; Nelz, R.; Sonusen, S.; Neu, E. *Crystals* **2017**, *7*, 124.

(2) Sukachev, D. D.; Sipahigil, A.; Nguyen, C. T.; Bhaskar, M. K.; Evans, R. E.; Jelezko, F.; Lukin, M. D. *Physical review letters* **2017**, *119*, 223602.

(3) Rogers, L. J.; Jahnke, K. D.; Teraji, T.; Marseglia, L.; Müller, C.; Naydenov, B.; Schauffert, H.; Kranz, C.; Isoya, J.; McGuinness, L. P.; Jelezko, F. *Nature Communications* **2014**, *5*, 4739 EP –.

(4) Neu, E.; Hepp, C.; Hauschild, M.; Gsell, S.; Fischer, M.; Sternschulte, H.; Steinmüller-Nethl, D.; Schreck, M.; Becher, C. *New J. Phys.* **2013**, *15*, 043005.

(5) Schröder, T.; Trusheim, M. E.; Walsh, M.; Li, L.; Zheng, J.; Schukraft, M.; Sipahigil, A.; Evans, R. E.; Sukachev, D. D.; Nguyen, C. T.; Pacheco, J. L.; Camacho, R. M.; Bielejec, E. S.; Lukin, M. D.; Englund, D. *Nature Communications* **2017**, *8*, 15376 EP –.

(6) Evans, R. E.; Sipahigil, A.; Sukachev, D. D.; Zibrov, A. S.; Lukin, M. D. *Physical Review Applied* **2016**, *5*, 044010.

(7) Marseglia, L.; Saha, K.; Ajoy, A.; Schröder, T.; Englund, D.; Jelezko, F.; Walsworth, R.; Pacheco, J. L.; Perry, D. L.; Bielejec, E. S.; Cappellaro, P. *Opt. Express* **2018**, *26*, 80–89.

(8) Jantzen, U.; Kurz, A. B.; Rudnicki, D. S.; Schäfermeier, C.; Jahnke, K. D.; Andersen, U. L.; Davydov, V. A.; Agafonov, V. N.; Kubanek, A.; Rogers, L. J.; Jelezko, F. *New Journal of Physics* **2016**, *18*, 073036.

(9) Shields, B. J.; Unterreithmeier, Q. P.; de Leon, N. P.; Park, H.; Lukin, M. D. *Phys. Rev. Lett.* **2015**, *114*, 136402.

(10) Han, K. Y.; Kim, S. K.; Eggeling, C.; Hell, S. W. *Nano Letters* **2010**, *10*, 3199–3203, PMID: 20698637.

(11) Harley, R. T.; Henderson, M. J.; Macfarlane, R. M. *Journal of Physics C: Solid State Physics* **1984**, *17*, L233.

(12) Redman, D.; Brown, S.; Rand, S. C. *J. Opt. Soc. Am. B* **1992**, *9*, 768–774.

(13) Dhomkar, S.; Zangara, P. R.; Henshaw, J.; Meriles, C. A. *Phys. Rev. Lett.* **2018**, *120*, 117401.

(14) Evans, R. E.; Bhaskar, M. K.; Sukachev, D. D.; Nguyen, C. T.; Sipahigil, A.; Burek, M. J.; Machielse, B.; Zhang, G. H.; Zibrov, A. S.; Bielejec, E.; Park, H.; Lončar, M.; Lukin, M. D. *Science* **2018**,

(15) Rose, B. C.; Huang, D.; Zhang, Z.-H.; Stevenson, P.; Tyryshkin, A. M.; Sangtawesin, S.; Srinivasan, S.; Loudin, L.; Markham, M. L.; Edmonds, A. M.; Twitchen, D. J.; Lyon, S. A.; de Leon, N. P. *Science* **2018**, *361*, 60–63.

(16) Nelz, R.; Fuchs, P.; Opaluch, O.; Sonusen, S.; Savenko, N.; Podgursky, V.; Neu, E. *Applied Physics Letters* **2016**, *109*, 193105.

(17) Nicolas, L.; Delord, T.; Huillery, P.; Neu, E.; Hétet, G. *AIP Advances* **2018**, *8*, 065102.

(18) Choi, S.; Leong, V.; Alagappan, G.; Krivitsky, L. *ACS Photonics* **2018**, *5*, 4244–4248.

(19) Neu, E.; Steinmetz, D.; Riedrich-Möller, J.; Gsell, S.; Fischer, M.; Schreck, M.; Becher, C. *New J. Phys.* **2011**, *13*, 025012.

(20) Aslam, N.; Waldherr, G.; Neumann, P.; Jelezko, F.; Wrachtrup, J. *New J. Phys.* **2013**, *15*, 013064.

(21) Siyushev, P.; Pinto, H.; Vörös, M.; Gali, A.; Jelezko, F.; Wrachtrup, J. *Phys. Rev. Lett.* **2013**, *110*, 167402.

(22) Dhomkar, S.; Jayakumar, H.; Zangara, P. R.; Meriles, C. A. *Nano Letters* **2018**, *18*, 4046–4052, PMID: 29733616.

(23) Tallaire, A.; Mayer, L.; Brinza, O.; Pinault-Thaury, M. A.; Debuisschert, T.; Achard, J. *Applied Physics Letters* **2017**, *111*, 143101.

(24) Chen, X.-D.; Li, S.; Shen, A.; Dong, Y.; Dong, C.-H.; Guo, G.-C.; Sun, F.-W. *Phys. Rev. Applied* **2017**, *7*, 014008.

(25) Ulbricht, R.; Van Der Post, S.; Goss, J.; Briddon, P.; Jones, R.; Khan, R.; Bonn, M. *Physical Review B* **2011**, *84*, 165202.

(26) Neu, E.; Agio, M.; Becher, C. *Opt. Express* **2012**, *20*, 19956–19971.

(27) Gali, A.; Maze, J. R. *Phys. Rev. B* **2013**, *88*, 235205.

(28) Thiering, G. m. H.; Gali, A. *Phys. Rev. X* **2018**, *8*, 021063.

(29) Meesala, S. et al. *Phys. Rev. B* **2018**, *97*, 205444.

(30) Arend, C.; Becker, J. N.; Sternschulte, H.; Steinmüller-Nethl, D.; Becher, C. *Physical Review B* **2016**, *94*, 045203.

(31) Afzelius, M.; Simon, C.; de Riedmatten, H.; Gisin, N. *Phys. Rev. A* **2009**, *79*, 052329.

(32) Claveau, S.; Bertrand, J.-R.; Treussart, F. *Micromachines* **2018**, *9*.